ADAPTIVE DETACHED EDDY SIMULATION OF ROTATING TURBULENT CHANNEL FLOW

Zifei Yin
Department of Aerospace Engineering
Iowa State University
Ames, IA, USA, 50010
zifeiyin@iastate.edu

Paul Durbin
Department of Aerospace Engineering
Iowa State University
Ames, IA, USA, 50010
durbin@iastate.edu

ABSTRACT

The Adaptive Detached Eddy Simulation model by Yin *et al.* (2015) allows eddies to be resolved near the wall if the mesh resolution is adequate. An element of this model is a lower bounding value (C_{lim}) of the model coefficient (C_{DES}), that is a function of grid resolution. The particular formula is designed to allow an approach to wall-resolved eddy simulation. The adaptive procedure, is capable of adapting to flow and geometry — in the present case, to rotational effects. In the current paper, fully developed rotating turbulent channel flow is studied to better understand the model performance. Simulations were performed at Rotation numbers ($2\Omega\delta/U_b$) ranging from 0.43 to 3.0, at $R_\tau = 180$, and from 0.167 to 1.5 at $Re_b = 14{,}000$. The normalized velocity profile is found to converge toward the laminar state as rotation increases. It does not completely laminarize, due to grid resolution being coarse compared to DNS.

INTRODUCTION

Simple, linear, scalar eddy viscosity Reynolds Averaged Navier Stokes (RANS) models, are incapable of accurately capturing flow rotational or streamline curvature effects. Extra corrections (Arolla & Durbin (2013), Spalart & Shur (1997)) to detect rotation and curvature need to be introduced to enhance/reduce eddy viscosity accordingly. Large Eddy Simulation responds to rotation and curvature directly through resolved stresses, and, hence, can more properly capture the physics in such flows. The capabilities of hybrid RANS/LES methods needs to be explored.

Detached Eddy Simulation, as a seamless, non-zonal, hybrid RANS/LES approach, that has shown great potential in predicting complex flows without extraordinary grid requirements. The original formulation was based on imposing a limit on a length scale in the *dissipation term*, so as to enhance turbulent dissipation. Away from walls, this reduces the eddy viscosity to a sub-grid viscosity.

An alternative to the original DES formula was proposed in Yin *et al.* (2015). In that formulation, grid spacing imposes a limit directly on the length scale in the eddy viscosity formula — rather than indirectly through the dissipation. To make it adaptive, the model constant, C_{DES}, is evaluated through the Germano-identity, and a lower bound imposed by an *ad-hoc* function of mesh resolution. The non-dimensional measure of resolution is defined as the ratio of grid size to Kolmogoroff scale. When the local mesh has LES resolution, the lower bound is deactivated to allow fully adaptive simulation. On a coarser meshes C_{DES} is bounded from below; and, on very coarse meshes it defaults to a constant value.

General flows with rotation and streamline curvature, are usually a combination of rotation, pressure gradient, and extra shear rate. To isolate rotational effects, experiments have been conducted on rotating channel flow (Johnston *et al.*, 1972; Nakabayashi & Kitoh, 1996; Maciel *et al.*, 2003; Nakabayashi *et al.*, 2004). The configuration is shown in figure 1. Under moderate rotation, one side of the channel has a tendency towards laminarization and the turbulence intensifies on the other. In the Navier-Stokes equations, the only change is the introduction of the Coriolis force term.

Rotating channel flow has been investigated by DNS at fairly low Reynolds number by Kristoffersen & Andersson (1993) and Grundestam *et al.* (2008). In Kristoffersen & Andersson (1993), rotation numbers up to 0.5 were simulated at $Re_\tau = 194$. In Grundestam *et al.* (2008), simulations were performed for rotation numbers from 0.98 to 3.0, at $Re_\tau = 180$, completing their earlier results at lower rotation numbers. These simulations have a limited domain size of $4\pi\delta \times 2\delta \times 2\pi\delta$, which according to Alvelius (1999), is not long enough to completely capture the very elongated structures occurring at low Rotation numbers. Lamballais *et al.* (1998) performed LES at higher Reynolds number. LES simulation of this flow by Piomelli & Liu (1995) was focused on testing subgrid models.

Whether it can capture relaminarization and how much flow physics it predicts are the two main questions to be answered by the current simulations.

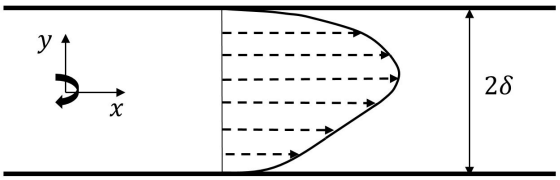

Figure 1. Sketch of rotating turbulent channel flow

MODEL FORMULATION

First, the adaptive DES model (Yin & Durbin, 2016) is summarized. The length scale formula

$$\ell_{DES} = \ell_{RANS} - f_d \max(0, \ell_{RANS} - \ell_{ES}) \tag{1}$$

is standard in DDES. Here

$$\ell_{RANS} = \frac{\sqrt{k}}{\omega}\ ; \quad \ell_{ES} = C_{DES}\Delta \tag{2}$$

and Δ is defined as

$$\Delta = (1 - f_d) * h_{max} + f_d * V^{1/3} \tag{3}$$

where V is the cell volume and $h_{max} = max(\Delta_x, \Delta_x, \Delta_x)$ is the maximum, local cell dimension. In the $\ell^2\omega$ formulation (Reddy *et al.*, 2014), this determines the eddy viscosity via

$$\nu_T = \ell_{DES}^2\, \omega \tag{4}$$

ω is the inverse turbulent time-scale of the $k-\omega$ model (equation 7). $\Delta = f_d * V^{1/3} + (1 - f_d)h_{max}$ interpolates between cube root of cell volume $V^{1/3}$ and maximum cell dimension h_{max}. Using $V^{1/3}$ rather than h_{max} in the eddy simulation region alleviates log-layer mismatch and emulates LES (Reddy *et al.*, 2014). Thus, on the eddy simulation branch ($f_d = 1$, $\ell_{ES} < \ell_{RANS}$), the subgrid viscosity becomes

$$\nu_T = (C_{DES}\Delta)^2\omega \tag{5}$$

which is similar to the Smagorinsky sub-grid viscosity $\nu_{SGS} = (C_s\Delta)^2|S|$.

f_d is the DDES shielding function (Spalart *et al.*, 2006),

$$\begin{aligned} f_d &= 1 - \tanh([8r_d]^3) \\ r_d &= \frac{k/\omega + \nu}{\kappa^2 d_w^2 \sqrt{U_{i,j}U_{i,j}}} \end{aligned} \tag{6}$$

where ν is the kinematic viscosity, κ the Von Karman constant, d_w the wall distance and $U_{i,j}$ the velocity gradient tensor. f_d ensures $\ell_{DES} = \ell_{RANS}$ near walls.

The DES formula for ν_T enters the production term of the k equation in the $k-\omega$ RANS model (Wilcox, 1998), with all the other terms unaltered;

$$\begin{aligned} \frac{Dk}{Dt} &= 2\ell_{DES}^2\omega|S|^2 - C_\mu k\omega + \nabla\cdot[(\nu + \sigma_k(k/\omega))\nabla k] \\ \frac{D\omega}{Dt} &= 2C_{\omega1}|S|^2 - C_{\omega2}\omega^2 + \nabla\cdot[(\nu + \sigma_\omega(k/\omega))\nabla\omega] \end{aligned} \tag{7}$$

The standard constants are $C_\mu = 9/100, \sigma_k = 1/2, \sigma_\omega = 1/2, C_{\omega1} = 5/9, C_{\omega2} = 3/40$.

It was shown by Yin *et al.* (2015) that an adaptive procedure can improve predictions. In their method, the dynamic procedure of LES (Lilly, 1992) is applied to the eddy viscosity (5). It uses the test-filtered tensors

$$\begin{aligned} L_{ij} &= -\widehat{\bar{u}_i\bar{u}_j} + \hat{\bar{u}}_i\hat{\bar{u}}_j \\ M_{ij} &= (\hat{\Delta}^2\hat{\bar{\omega}}\hat{\bar{S}}_{ij} - \Delta^2\widehat{\bar{\omega}\bar{S}_{ij}}) \end{aligned} \tag{8}$$

The notations used in (8) are the same as in Lilly (1992). The tensor L_{ij} is a stress computed from the resolved field of turbulence. The hat denotes explicit test filtering, with a filter width that is twice the grid scale. The test filter is a spatial average of data in neighboring cells, weighted by the surface area of the common face.

There is one other aspect to the adaptive procedure: in order for the test filter to be valid, a significant portion of the inertial range needs to be resolved. But the coarse meshes that sometimes are used in DES do not capture enough of the small scales. For this reason a lower bound is placed on on the computed value of C_{DES}

$$\begin{aligned} C_{DES} &= \max(C_{lim}, C_{dyn}) \\ C_{dyn}^2 &= \max\left(0, \frac{L_{ij}M_{ij}}{2M_{ij}M_{ij}}\right) \end{aligned} \tag{9}$$

where the lower limit is determined by the empirical formula (Yin & Durbin, 2016)

$$\begin{aligned} C_{lim}(\xi) =& 0.06(max(min(\xi - 23)/7, 1), 0) \\ &+ max(min(\xi - 65)/25, 1), 0)) \end{aligned} \tag{10}$$

The argument compares grid spacing to the Kolmogoroff scale $\xi = h_{max}/\eta$. An estimate of dissipation is needed to construct the Kolmogoroff scale.

$$\varepsilon = C_\mu k\omega, \qquad \eta = \left(\frac{\nu^3}{\varepsilon}\right)^{1/4} \tag{11}$$

If the grid is coarse, formula (10) limits to a default value of 0.12 (Reddy *et al.*, 2014). If the local grid has LES resolution, the limiting value approaches zero. Equation 11 returns $\varepsilon = 0$ in laminar flow ($k = 0$), with the corresponding evaluated Kolmogoroff scale to be infinity - this yields $C_{lim} = 0$. $\eta \to 0$ also implies that no Kolmogoroff scale exists in laminar flow.

The adapted C_{DES} value, obtained from equation (9), is used in equation (1) and, hence, in ν_T; and thereby, in the production of turbulent kinetic energy. If the adaptive procedure makes C_{DES} small, the production of k will be small and the subgrid viscosity can become very small.

SIMULATION

The open source code OpenFOAM (Jasak *et al.*, 2007) was used for all the present computer simulations. Gaussian finite volume integration, with central differencing for interpolation, was selected for spatial discretization. The Sweby limiter was applied on convection terms in the k and

ω equations. Time integration was by 2^{nd} order, backward finite differences. An adjustable time step was used to ensure that the maximum CFL number in the flow is 0.1.

Rotation is represented by adding the Coriolis force in the momentum equations. *No rotational corrections were made* to the $k-\omega$ model. Periodic boundary conditions, with uniform pressure gradient are applied to insure the prescribed friction velocity Reynolds number.

The non-dimensional measure of rotation is the *Rotation number*, defined as $Ro = 2\Omega\delta/U_b$, corresponding to the inverse of the *Rossby* number., where U_b is the bulk velocity, δ the channel half-width, and Ω the angular frequency. In our simulations at $Re_\tau = 180$, U_b was specified for each *Rotation* number (0, 0.43, 0.77, 0.98, 1.50, 2.06, 2.49, 3.0), the molecular viscosity is adjusted to match target Re_τ. In another simulation at $Re_b = 14,000$, following LES reference data, the bulk velocity and molecular viscosity are kept same. As a result, Re_τ changes with *Rotation* number (0, 0.167, 0.5, 1.5).

0.1 Channel flow at $Re_\tau = 180$

Current simulations correspond to the DNS study of Grundestam *et al.* (2008), and their earlier simulations with $Ro = 0.43$ and 0.77 (Alvelius, 1999). Due to the asymmetry in the velocity profile, the average friction velocity u_τ is targeted to match the DNS value. Note that the separate friction velocities, on the stable and unstable sides of the channel, will not be exactly the same as the DNS if the velocity profiles don't match.

The domain of the computation has dimensions of $4\pi\delta \times 2\delta \times 2\pi\delta$ in streamwise, wall normal, and spanwise directions, respectively. It is the same as the DNS (Grundestam *et al.*, 2008). The DES grid contains $80 \times 80 \times 40$ cells in streamwise, wall normal, and spanwise directions. The grid resolution is $\Delta x^+ = \Delta z^+ \approx 30$, estimated from the average friction velocity. Similarly y^+ is 0.6 at the first cell, and reaches 14 at channel center. While this is about 3 times coarser in each direction than the DNS, the DNS used a pseudo-spectral method, so the effective coarseness is a bit higher than this. In the DNS of Grundestam *et al.* (2008), the number of cells in the wall normal direction was increased from 128 at low *Ro*, to 200 at high *Ro*, to ensure a numerically converged solution. In the current DES, only 80 were used. It will be seen in the following results that less grid resolution might affect predictions at the highest Rotation numbers.

The rotation affects friction velocities by increasing u_τ^u on the unstable side and decreasing u_τ^s on the stable side. Wall friction velocities normalized by the average, are plotted in figure 2. The DES agrees quite well with the DNS at low Rotation number ($Ro < 1$). DES captures the maximum difference of shear velocities, at $Ro \approx 0.43$. With increasing Rotation number, DNS shows monotonic convergence of friction velocities to unity, as the channel approaches, symmetric laminar flow. At $Ro = 3.0$, the flow is fully laminar and exactly symmetric. Full laminarization is not captured the DES model, with the current grid resolution.

Figure 3 compares time averaged velocity profiles to DNS data. Asymmetric velocity profiles are captured and are in perfect agreement with DNS at low Rotation numbers. Comparison is also made with non-adaptive DES model, where $C_{DES} = 0.12$ globally (data from Yin *et al.* (2015)). The adaptability of C_{DES} shows significant improvement over a global constant on velocity profiles. The non-adaptive model deviates from DNS even at low *Ro*. De-

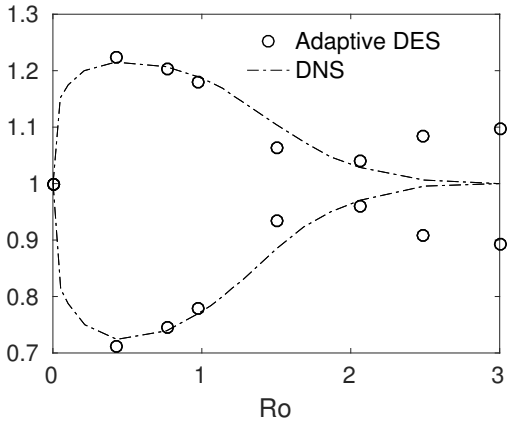

Figure 2. Ratios u_τ^u/u_τ and u_τ^s/u_τ for different Rotation numbers predicted by DES, compared to DNS

viation from DNS starts at $Ro = 0.98$, consistent with figure 2. At higher *Ro*, the velocity of the adaptive DES model is over predicted on the stable side. However, the slope of velocity profile on the unstable side still follows DNS predictions (the shear is 2Ω towards the center of the channel).

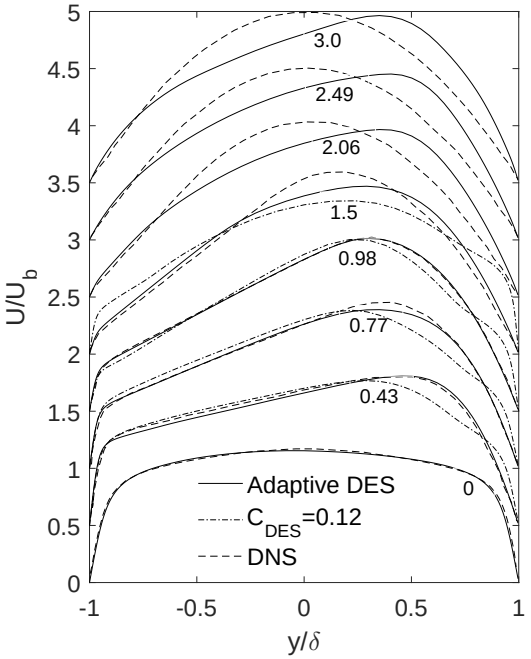

Figure 3. DES computed U/U_b compared to DNS at $Ro =$ 0, 0.43, 0.77, 0.98, 1.50, 2.06, 2.49, and 3.0. $Ro = 0$ on the bottom and 3.0 on the top, each shifts by 0.5 along y-axis.

The stable side, where the flow tends to relaminarize at large Rotation number, is where DES predictions become incorrect. The culprit is revealed in figure 4, where turbulent stresses are observed on the stable side, when the DNS shows them to nearly vanish.

The spurious behavior of the DES computation may be *partially* attributed to lack of resolution. Adaptive DES adjusts C_{DES} toward zero, driving the subgrid viscosity to low

values. Then the near-wall region becomes a DNS, on the stable side. In Grundestam *et al.* (2008), the number of cells in the wall normal direction was increased from 128 to 160 at $Ro = 1.27$ and again to 200 at $Ro = 1.87$ to ensure 'numerically converged solutions'. However, the current grid, which has only 80 cells in wall normal direction, can't guarantee prediction of complete relaminarization, let alone the resolutions in streamwise and spanwise are just 36% and 25% of DNS. The result has undesired fluctuations on the stable side, overestimating turbulent mixing. This pulls the peak velocity toward the stable side. Thus, the failure of DES at high Rotation number is not due to the model, it is due to the mesh.

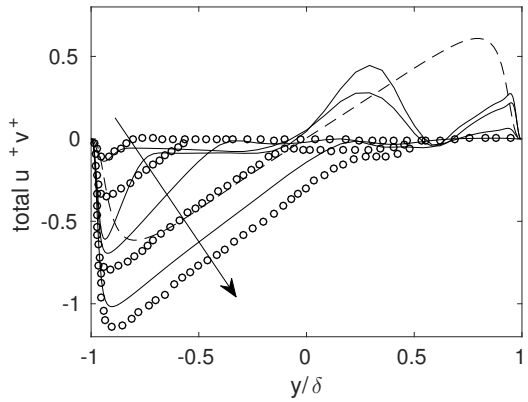

Figure 4. DES predicted total (Resolved+Modeled) u^+v^+ at $Ro = 0.98, 1.5, 2.06, 2.49$ (solid line) and $Ro = 0$ (dashed line), compared to DNS (circles). Arrow indicates increasing Rotation number.

Total (resolved + modeled) Reynolds shear stress profiles are plotted in figure 4. As has been mentioned, on the stable side ($y/\delta > 0$), undesired fluctuations exist. However, the correct trend of Reynolds shear stress on the unstable side is captured: compared to $Ro = 0$, the Reynolds shear stress decreases under weak rotational and then increases to even higher magnitude under strong rotation. Note that the average Reynolds number is kept at $Re_\tau = 180$, to match the DNS value. But at high Ro, the friction velocity on each side does not match the DNS value, which may account for the underestimation of normalized total u^+v^+ in figure 4.

Figure 5 shows time averaged eddy viscosity ratio (ν_t/ν) versus rotation speed. On the unstable side, viscosity ratio increases at low Ro, when turbulence is enhanced on this side, then decreases due to the tendency toward relaminarization. On the stable side, eddy viscosity ratio monotonically decreases with increasing Ro, correctly approaching zero. At $Ro = 2.06$, the whole domain is essentially a DNS. *At this and higher rotation rates, the simulation is no longer a test of DES.*

Figure 6, shows the time averaged, dynamic constant C_{DES}. C_{DES} shares the same trend with eddy viscosity ratio. On the unstable side, C_{DES} increases and then decreases with increasing Ro. On the stable side, the C_{DES} becomes low, though not zero. This reflects the presence of test-filter scale motions, due to grid coarseness. It is not problematic, because, as the subgrid viscosity has become zero, there is no basis for adaptivity.

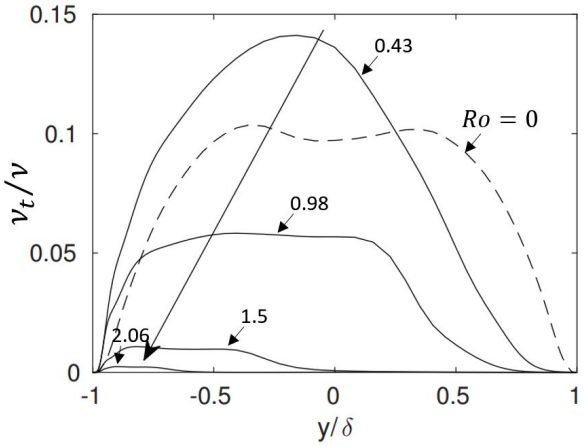

Figure 5. Averaged eddy viscosity ratio (ν_t/ν) at $Ro = 0.43$, 0.98, 1.5, 2.06 (solid line), compared to $Ro = 0$ (dashed line). Arrow indicates increasing Rotation number.

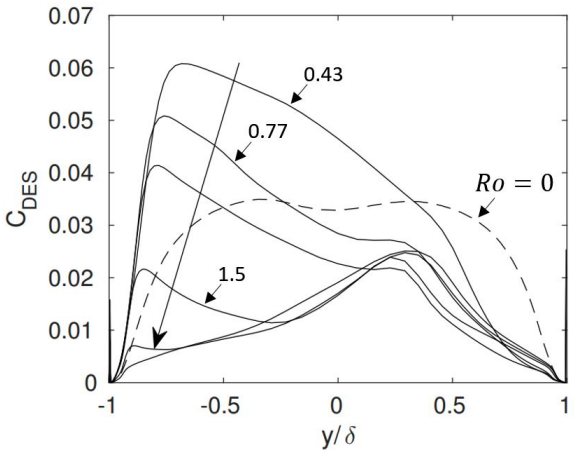

Figure 6. Averaged C_{DES} at $Ro = 0.43$, 0.77, 0.98, 1.5, 2.06, 2.49 (solid line), compared to $Ro = 0$ (dashed line). Arrow indicates increasing Rotation number.

Table 1 lists Reynolds number based on bulk velocity. Up to $Ro = 0.98$, DES is very close to DNS. For higher Ro, although the averaged Re_τ matches DNS, failure to predict laminar flow on the stable side causes Re_b to deviate from DNS. Similar behavior is also observed in friction velocities: up to $Ro = 0.98$, the DES prediction is within 1% of DNS predictions. After that, discrepancy with DNS increases with Ro. The final symmetric, laminar, friction velocities observed in DNS at $Ro = 3$ are not captured by DES.

Table 1. DES predicted Reynolds number based on bulk velocity ($Re_b = U_b\delta/\nu$) and shear velocities (Re^s_τ, Re^u_τ)

Ro	Re_b	Re^s_τ	Re^u_τ
0.43	2857	127.8	220.2
0.77	3278	133.7	216.0
0.98	4016	139.6	211.7
1.50	5952	170.7	188.9

0.2 Channel flow at $Re_b = 14,000$

This section corresponds to the LES of Lamballais *et al.* (1998). In that simulation, the Reynolds number is 14,000, based on bulk velocity. The Rotation numbers are 0.167, 0.5, and 1.5, resulting $Re_\tau = 361$, 317 and 223, respectively. The current grid has $128 \times 97 \times 64$ cells in a domain of $2\pi\delta \times 2\delta \times \pi\delta$ — the same as in the LES. Estimating from the non-rotating case, the grid has a resolution of $\Delta X^+ = 2\Delta Z^+ = 20$, with ΔY^+ ranging from 0.65 adjacent to wall, to 30 at channel centerline.

Predicted velocity profiles are plotted in figure 7. The adaptive model correctly predicts the region of linear slope equal to 2Ω, and agrees with LES. However, at higher rotation number (1.5), DES does not predict the same velocity peak as shown in LES. Grid resolution that partially accounts for velocity deviation from DNS at $Re_\tau = 180$ can not explain the disagreement here. Intrinsically, by adopting the dynamic procedure, the DES model should perform like the dynamic Smagorinsky model away from wall. A possible explanation could be, using ω to substitute $|S|$ somehow deteriorates the prediction accuracy.

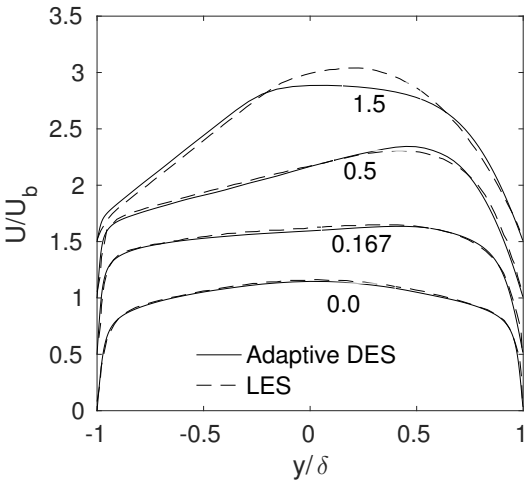

Figure 7. DES computed U/U_b compared to LES at $Ro = 0$, 0.167, 0.5, and 1.5. Each shifts by 0.5 along y-axis.

Table 2 shows the computed friction velocity based Reynolds number. The trend reported for the LES is captured in the current simulations. Friction velocities u_τ^u and u_τ^s are normalized by the u_τ^0 of non-rotating flow. It is consistent with LES that the friction on the unstable side first increases under the rotational effect and then decreases under the tendency toward relaminarization.

Figure 8 compares DES predictions of streamwise u_{rms} to LES. Overall, good agreement is achieved. The underestimation of u_{rms} near $y/\delta = 1$ at $Ro = 0.167$ may be a result of using RANS length scales near the wall. When $Ro = 1.5$, u_{rms} is small across the whole channel due to suppression of turbulence by rotational effect.

CONCLUSION

Rotating channel flows with Ro ranging from 0.43 to 3.0 at $Re_\tau = 180$ and higher are tested using the Adaptive Detached Eddy Simulation model. Good agreement with DNS and LES is achieved under moderate Rotation number

Table 2. DES predicted Reynolds number based on friction velocity

Ro	Re_τ	u_τ^u/u_τ^0	u_τ^s/u_τ^0
0.00	389	1.0	1.0
0.167	372	1.17	0.67
0.50	338	1.10	0.54
1.50	224	0.66	0.48

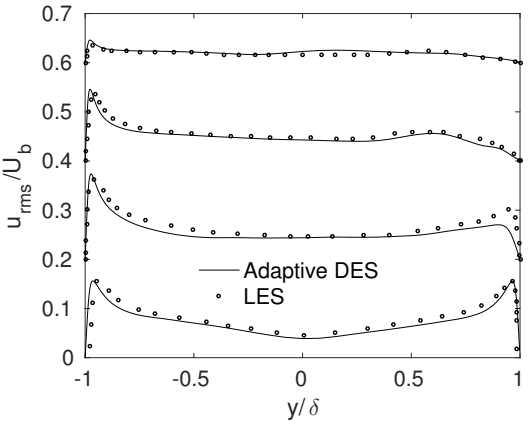

Figure 8. DES computed u_{rms}/U_b compared to LES at $Ro = 0$ (bottom), 0.167, 0.5, and 1.5 (top). Each shifts by 0.2 along y-axis.

($Ro < 1$). However, the result is only qualitatively correct at high Ro. The adaptive procedure successfully responds to rotational stabilization and reduces the subgrid viscosity. Thus, relaminarization drives the subgrid viscosity to zero, making the simulation more like DNS than DES. Deviation from DNS may partially be explained by inadequate grid resolution for DNS. It is possible that using ω rather than $|S|$ may deteriorate predictive accuracy, but the dynamic procedure is expected to minimize such difference.

Overall, the current set of rotating channels shows how DES, with the adaptive procedure, is capable of adjusting the model constant and subgrid viscosity according to flow characteristics. The underlying $k-\omega$ model was not modified, so it has no dependence on rotation; rotational effects are captured only by the resolved eddies. The thickness of the shielded, RANS region, is also decreased, allowing eddy resolving in the vicinity of the solid boundary. Without adaptivity, a RANS region would exist near the wall (Yin *et al.*, 2015), in which rotation effects would not be captured.

REFERENCES

Alvelius, Krister 1999 Studies of turbulence and its modelling through large eddy- and direct numerical simulation. PhD thesis, Royal Institute of Technology.

Arolla, Sunil K & Durbin, Paul A 2013 Modeling rotation and curvature effects within scalar eddy viscosity model framework. *International Journal of Heat and Fluid Flow* **39**, 78–89.

Grundestam, Olof, Wallin, Stefan & Johansson, Arne V

2008 Direct numerical simulations of rotating turbulent channel flow. *Journal of Fluid Mechanics* **598**, 177–199.

Jasak, Hrvoje, Jemcov, Aleksandar, Tukovic, Zeljko *et al.* 2007 Openfoam: A c++ library for complex physics simulations. In *International workshop on coupled methods in numerical dynamics*, , vol. 1000, pp. 1–20. IUC Dubrovnik, Croatia.

Johnston, James P, Halleent, Robert M & Lezius, Dietrich K 1972 Effects of spanwise rotation on the structure of two-dimensional fully developed turbulent channel flow. *Journal of Fluid Mechanics* **56** (03), 533–557.

Kristoffersen, Reidar & Andersson, Helge I 1993 Direct simulations of low-reynolds-number turbulent flow in a rotating channel. *Journal of fluid mechanics* **256**, 163–197.

Lamballais, Eric, Métais, Olivier & Lesieur, Marcel 1998 Spectral-dynamic model for large-eddy simulations of turbulent rotating channel flow. *Theoretical and computational fluid dynamics* **12** (3), 149–177.

Lilly, Douglas K 1992 A proposed modification of the germano subgrid-scale closure method. *Physics of Fluids A: Fluid Dynamics (1989-1993)* **4** (3), 633–635.

Maciel, Yvan, Picard, Donald, Yan, Guorong, Dumas, G & Gleyzes, C 2003 Fully developed turbulent channel flow subject to system rotation. *AIAA Paper* **4153**.

Nakabayashi, Koichi & Kitoh, OSAMI 1996 Low reynolds number fully developed two-dimensional turbulent channel flow with system rotation. *Journal of Fluid Mechanics* **315** (1), 1O29.

Nakabayashi, Koichi, Kitoh, Osami & Katoh, Yoshitaka 2004 Similarity laws of velocity profiles and turbulence characteristics of couette–poiseuille turbulent flows. *Journal of Fluid Mechanics* **507**, 43–69.

Piomelli, Ugo & Liu, Junhui 1995 Large-eddy simulation of rotating channel flows using a localized dynamic model. *Physics of Fluids (1994-present)* **7** (4), 839–848.

Reddy, KR, Ryon, JA & Durbin, PA 2014 A ddes model with a smagorinsky-type eddy viscosity formulation and log-layer mismatch correction. *International Journal of Heat and Fluid Flow* **50**, 103–113.

Spalart, PR & Shur, M 1997 On the sensitization of turbulence models to rotation and curvature. *Aerospace Science and Technology* **1** (5), 297–302.

Spalart, Philippe R, Deck, Shur, Shur, ML, Squires, KD, Strelets, M Kh & Travin, A 2006 A new version of detached-eddy simulation, resistant to ambiguous grid densities. *Theoretical and computational fluid dynamics* **20** (3), 181–195.

Wilcox, David C 1998 *Turbulence modeling for CFD*, , vol. 2. DCW industries La Canada, CA.

Yin, Zifei & Durbin, Paul A 2016 An adaptive des model that allows wall-resolved eddy simulation. *Int. J. Heat and Fluid Flow* $HFF_2016_168_R1$ (to appear).

Yin, Zifei, Reddy, Karthik & Durbin, Paul A 2015 On the dynamic computation of the model constant in delayed detached eddy simulation. *Physics of Fluids (1994-present)* **27** (2), 025105.